

High-Performance CuInS_2 Quantum Dot Laminated Glass Luminescent Solar Concentrators for Windows

Matthew R. Bergren,^{†,§} Nikolay S. Makarov,^{†,§} Karthik Ramasamy,[†] Aaron Jackson,[†] Rob Guglielmetti,[‡] and Hunter McDaniel^{*,†,§}

[†]UbiQD, Inc., Los Alamos, New Mexico 87544, United States

[‡]National Renewable Energy Laboratory, Golden, Colorado 80401, United States

S Supporting Information

ABSTRACT: Building-integrated sunlight harvesting utilizing laminated glass luminescent solar concentrators (LSCs) is proposed. By incorporating high quantum yield (>90%), NIR-emitting $\text{CuInS}_2/\text{ZnS}$ quantum dots into the polymer interlayer between two sheets of low-iron float glass, a record optical efficiency of 8.1% is demonstrated for a 10 cm × 10 cm device that transmits ~44% visible light. After completing prototypes by attaching silicon solar cells along the perimeter of the device, the electrical power conversion efficiency was certified at 2.2% with a black background and at 2.9% using a reflective substrate. This “drop-in” LSC solution is particularly attractive because it fits within the existing glazing industry value chain with only modest changes to typical glazing products. Performance modeling predicts >1 GWh annual electricity production for a typical urban skyscraper in most major U.S. cities, enabling significant energy cost savings and potentially “net-zero” buildings.



According to the International Energy Agency (IEA), worldwide installed solar energy capacity has grown dramatically, reaching >300 GW by the end of 2016—more than double the installed capacity from 2013.¹ Although the growth is impressive, photovoltaics (PVs) currently account for just 1.8% of the worldwide electricity supply and even less in the United States (~1.3%). The IEA projects that by 2050 PVs will account for 27% of electricity generated worldwide.¹ To achieve that projection, new and innovative technology is needed to harvest sunlight for electricity in densely populated areas. One major barrier to entry into urban markets, where electricity demand (and price) is high, is the lack of solar real estate—an area to install PV. Tall buildings utilize large amounts of electricity² but lack enough rooftop space or other nearby areas to mount solar panels. Urban electricity is generally produced by fossil fuel burning power plants outside of city limits and then is transferred using the electric grid, which is one reason why urban electricity is more expensive compared to rural areas. For example, in June 2017, New York households paid 18.8 cents per kWh for electricity, 42% higher than the U.S. national average of 13.2 cents per kWh.³

Partially transparent luminescent solar concentrators (LSCs) provide a simple and cost-effective strategy for harvesting sunlight using windows to generate electricity. Unlike other

solar window technologies, such as semitransparent solar cells, well-designed LSC-equipped insulating glass units (IGUs) fit within the existing IGU supply chain at the raw material level. As a result, LSC windows are expected to cost less to manufacture and have faster market adoption compared to other solar window technologies. More importantly, LSCs provide high-quality viewing aesthetics because they do not require electrical interconnects on the plane of the window (only at the edges) and offer a wide variety of color and tint options. An LSC typically consists of a single transparent surface (e.g., glass or plastic) that is coated with emissive chromophores, such as organic dyes or quantum dots (QDs).^{4,5} Incident sunlight (direct or diffused) is absorbed by the chromophores and re-emitted at a longer wavelength. The emitted light then propagates to the edges of the LSC by total internal reflection and is converted into electricity by PV cells installed along the perimeter of the LSC.

In this Letter, we report a new LSC design that utilizes a laminated glass configuration whereby a polymer interlayer, embedded with QD chromophores, is sandwiched between two

Received: December 29, 2017

Accepted: January 30, 2018

Published: January 30, 2018

panes of glass. This new LSC design, coupled with highly emissive, near-infrared (NIR) $\text{CuInS}_2/\text{ZnS}$ QDs resulted in a high optical efficiency of 8.1% and a National Renewable Energy Laboratory (NREL) certified power conversion efficiency (PCE, efficiency of converting sunlight to electricity) of 2.94 and 2.18%, (with and without a reflective substrate), while transmitting 43.7% of visible light and absorbing only 35.5% of the AM1.5 solar spectrum.

While the LSC concept was originally introduced in the 1970s,^{6,7} organic dyes were used as the luminescent chromophores. However, organic dyes typically suffer from large self-absorption losses (large overlap between absorption and emission spectra),⁶ have poor stability,^{8,9} are narrow-band absorbers, and typically are not spectrally matched with the peak external quantum efficiency (EQE) of the solar cells. For these reasons, LSCs based on semiconductor QDs have been recently proposed.^{10–18}

QDs offer several additional advantages over the traditional organic chromophores used in LSC applications, such as a wider spectral absorption range, straightforward tunability of the emission, and potential for color neutrality of the tinted windows.^{15,16} Unfortunately, most QDs are not well suited for use in LSCs due to high manufacturing costs and toxicity issues^{10,13,14} or do not exhibit bright NIR emission and/or large Stokes shift,¹⁶ which is required for power performance and aesthetic reasons. One composition of QD that overcomes these issues is CuInS_2 .¹⁸ These nanomaterials can be manufactured using a low-cost, simple heat-up method, do not suffer from toxicity issues, have a large Stokes shift, and can be fabricated with near-100% photoluminescence (PL) quantum yield (QY) in the NIR spectral range.^{18–20}

In this study, we utilize $\text{CuInS}_2/\text{ZnS}$ QDs with a PL peak at ~ 1.44 eV (862 nm), which is well-matched with the peak EQE of crystalline silicon (c-Si) solar cells (~ 850 – 950 nm), and exhibited a PL QY of 91% when dispersed in nonpolar solvents. The QDs were synthesized based on the methods reported in refs 19 and 20. Figure 1a shows the absorption and PL spectra (measured in toluene) for the NIR QDs used in this study. The QD band-edge can be identified by the location of the broad shoulder observed in the absorption spectrum at ~ 2.0 eV, which, compared to the emission peak of ~ 1.44 eV, demonstrates a very large Stokes shift for these materials (>550 meV). This has practical implications for the final LSC device as it shows that the QDs have very little self-absorption and thus minimal intrinsic optical losses.

One promising way to integrate LSC technology into existing window manufacturing processes is to have the emissive-nanocomposite be an interlayer for laminated glass, which is commonly known as safety glass. In this form factor, the polymer is sandwiched between two pieces of glass and located in the outermost pane of the IGU (Figure 1b). Similar to typical LSCs, if the nanocomposite interlayer is not optimized, then the LSC will suffer from increased losses due to scattering (haze from polymer impurities or QD aggregation), reabsorption (self-absorption or polymer absorption),¹⁶ and/or larger escape cones (from textured surfaces). By laminating the nanocomposite between two sheets of optically clear glass, most of the waveguide and the external surfaces are composed of flat glass, which reduces the optical requirements for the polymer and decreases optical losses for the device. Additionally, in typical safety glass, the interlayer thickness ranges between 30 and 90 mil, which composes only ~ 6 – 18% of the total thickness of the laminated glass for 1/4 in.-thick panes.

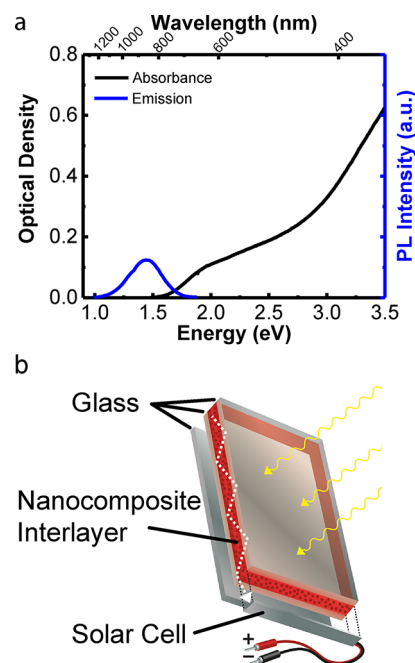


Figure 1. (a) Absorption and PL spectra for NIR-emitting $\text{CuInS}_2/\text{ZnS}$ QDs in toluene. (b) Diagram of the laminated glass LSC design.

Because most of the light will propagate through the glass, we first compared the optical performance of traditional (green colored) float glass with low-iron and no-iron glass (see the Supporting Information, Table S1). The low-iron glass demonstrated a 3 \times improvement in optical efficiency over the traditional float glass, and therefore, this study is focused on prototyping LSCs with low-iron float glass.

While numerous papers report characterization of LSCs, each of the groups prefers their own metric, which makes comparing the results between each other difficult. For example, in ref 10, the authors report a PCE of 2.8% for a small LSC (area of 15.4 cm^2) composed of toxic CdSe-based core/shell QDs absorbing less than 50% of the solar spectrum. They also predict that the PCE drops down to $<1\%$ for a 50 cm \times 50 cm device. Reference 15 reports an optical power efficiency of 3.2% for a 12 cm \times 12 cm LSC based on $\text{CuInSe}_{x-1}\text{S}_x/\text{ZnS}$ QDs. The optical power efficiency, however, refers to the optical efficiency of the LSC ($\eta_{\text{Opt}} = \text{photons emitted from LSC edge} / \text{incident excitation photons}$; see the Supporting Information for more details) and not to the PCE, which is calculated from current vs voltage measurements (I – V). More recently, the authors in ref 18 report an optical efficiency of 5.7% for the 7.5 cm \times 7.5 cm LSC based on $\text{CuInS}_2/\text{CdS}$ QDs; however, they do not provide details on the absorption of the solar spectrum, which directly affects the measured values of PCE and η_{Opt} because LSCs are partially transparent.

All of these values are well below one of the highest-performing dye-based LSCs²¹ with a reported PCE of 7.1%. However, this 5 cm \times 5 cm LSC utilizes two organic dyes with small Stokes shifts, and therefore, performance would drop precipitously with LSC size. A tandem LSC was also recently demonstrated using QDs by Wu et al., with an optical power efficiency of 6.4%, a PCE of 3.1%, and a low visible light transmittance (VLT) of 23%. In Table 1, we summarize these and others various LSC efficiencies and compare LSCs performance to this work.

Table 1. Comparison of Various LSC Efficiencies

ref	fluorophore	emission QY (%)	LSC size $L \times W$ (cm ²)	optical efficiency (%)	PCE (%)	solar abs* (%)	VLT* (%)
This work ^a	CuInS ₂ /ZnS QDs	91 (66% film)	10 × 10	8.1	2.94	35.5	43.7
This work ^b	CuInS ₂ /ZnS QDs	91 (66% film)	10 × 10	8.1	2.18	35.5	43.7
21 ^c	Lumogen F Red305		5 × 5		7.1		
	Fluorescence Yellow CRS040						
22 ^d	CuInSe ₂ /ZnS QDs	72	15.2 × 15.2	6.4	3.1	24.0	~30.0
	Mn: Cd _{1-x} Zn _x S/ZnS QDs	78				4.6	
18	CuInS ₂ /CdS QDs	75	7.5 × 7.5	5.7			
22	CuInSe ₂ /ZnS QDs	72	15.2 × 15.2	5.5	2.5	28.0	23.0
15	CuInSe _x S _{2-x} /ZnS QDs	40	12 × 12	3.3		10.0	
16	Si QDs	50	12 × 12	2.9			70.0
10 ^e	CdSe/CdS/CdZnS/ZnS QDs	45	4.95 × 3.1	na	2.8	31.0	
23 ^f	CdSe/Cd _{1-x} Zn _x S QDs	70	10.2 × 10.2	1.9		6	
24 ^g	CdSe/Cd _x Pb _{1-x} S QDs	40	7 × 1.5	1.4	1.15		
25 ^h	PbS/CdS QDs	40–50	2 × 1.5	6.1			
25 ^h	PbS/CdS QDs	40–50	10 × 1.5	1.1			
26 ⁱ	CdSe/CdS QDs	45	21.5 × 1.35	0.6			

^aPCE measured with a reflective substrate below the LSC. ^bPCE measured with a nonreflective substrate below the LSC. ^cDiffusive reflector substrate below the LSC. ^dTandem (2 layers) LSC. ^eThree edges of the LSC slab terminated with mirrors. Diffusive white reflective substrate used. ^fSilica-coated QD used; 25% transmission at 405 nm. ^gThree edges and the bottom of the LSC terminated with mirrors. ^hThree edges of the LSC terminated with mirrors. ⁱWhite diffuse reflectors placed in the proximity of the long edges of the LSC. *Values are reported without a reflective/nonreflective/diffusive substrate.

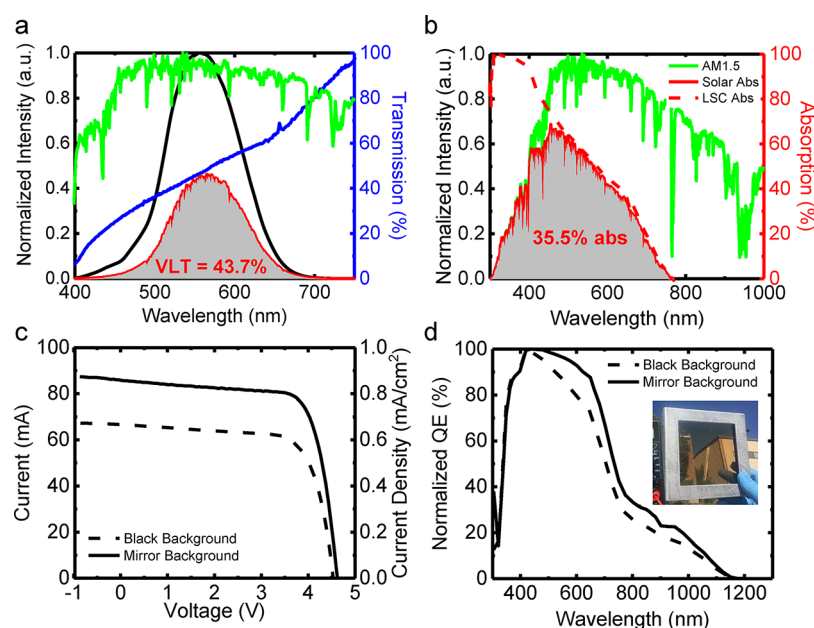


Figure 2. (a) VLT spectra of the NIR-QD LSC glass laminate. The VLT curve (red) was produced by convolution of the human eye photopic response (black) with the sample's transmittance (blue) and the normalized solar spectrum (green). The total VLT was then calculated by taking the ratio of the integrated areas of the VLT and the photopic response curve. (b) Calculated solar absorption (red) for the LSC taken from the convolution of the solar spectrum (green) and the absorption of the window (red dash). (c) NREL certified I – V curves measured under AM1.5 illumination in a solar simulator for LSC with an absorbing black background (dashed line) and a mirrored background behind the window (solid line), simulating a low-e coating. The corresponding current density values are shown on the right axis, which were calculated by dividing the current by the device's active area (99.73 cm²). (d) Normalized quantum efficiency measured and averaged from four locations on the device for both a black and mirrored background. The inset shows a photo of the LSC device.

In order to build an efficient LSC device and achieve the best combination of environmental stability, low self-absorption, high PL QY, and spectrally matched emission with Si solar cells, we used the glass laminate design described in the previous section. The laminated glass LSC was 11 cm × 11 cm and fabricated with an acrylate nanocomposite interlayer that contained 860 nm emitting CuInS₂/ZnS QDs at a loading of 0.4 wt %. The acrylate-based interlayer was made by a

procedure similar to that in refs 10 and 15. The interlayer was then sandwiched between two sheets of low-iron float glass (Krystal Klear glass manufactured by Asahi Glass Company). The QD loading was chosen to achieve ~50% VLT, which takes into account the amount of light absorbed in the region of the spectrum where the human eye is sensitive. To calculate the VLT (Figure 2a), the transmittance of the sample is measured (blue line) and then convoluted with the photopic response of

the human eye (black line) and the normalized AM1.5 solar spectrum (green line). The VLT is then calculated by taking the ratio of the integrated area of the convoluted curve (red line) with the integrated area of the photopic response of the eye. For the LSC described in this work, we calculated a VLT of 43.7%, which is slightly more absorbing than the target 50%.

Another way to characterize how much light is transmitted through the window (required to compute η_{Opt}) is to measure the solar absorption (A) of the window (Figure 2b, red line). To calculate this value, the absorbance ($A = 1 - 10^{-\text{OD}}$, dashed red line) is convoluted with the normalized AM1.5 solar spectrum (green line), and then, the ratio of the integrated areas of the solar absorption and the normalized solar spectrum is taken. For this LSC, the solar absorption was calculated to be 35.5%.

Before attaching solar cells to the perimeter of the LSC, the QY and haze of the nanocomposite were measured, and the theoretical optical efficiency was calculated for the glass laminate (see the Supporting Information). We found that the QY of the QDs embedded in the nanocomposite dropped to 66% and the haze of the LSC was 1.6% at 640 nm. Using the measured optical values, we obtain a maximum theoretical optical efficiency of 17% for this device, if we assume that there are negligible losses from reabsorption and scattering (see the Supporting Information). We then measure η_{Opt} at several wavelengths using LED floodlamps and a Thorlabs PM100USB power meter and S120VC sensor to obtain the spectrally integrated optical efficiency and compare it to the theoretical value above.

The measured η_{Opt} was as high as 9% in the blue spectral region and as low as 7% in the red. Spectrally integrated optical efficiency of the LSC was measured at 8.1%, which is about half of the 17% predicted by theory but still the highest η_{Opt} reported to date for a LSC (single or tandem). One can argue that the calculated theoretical value might not be applicable to the LSC due to contribution from reabsorption losses, but the overlap integral between the absorption spectrum and normalized emission spectrum is below 0.003. Given that the ratio of the length and thickness of the LSC (L/d) is ~ 71.4 , the denominator of the equation (eq S1) is 1.25, and thus the predicted optical efficiency should be at least 14%. The relatively high haze of the LSC is likely responsible for the deviation of the measured optical efficiency from the predicted value.

To characterize the electrical PCE of the device, polycrystalline Si solar cells manufactured by Aoshike, having an estimated PCE of 11% (for AM1.5), were attached to the perimeter of the QD-LSC glass laminate using an optical epoxy and wired in series. The completed device, which had active area of 10 cm \times 10 cm (99.73 cm² as defined by a metal mask) was then sent to the NREL in order to measure a certified PCE as well as the device's EQE. The I - V and EQE were measured at 25 °C under an ASTM G173 global spectrum, which had an irradiance of 1000 W/m². The PCE and EQE were then measured for the sample in two different configurations: first, a nonreflective black absorbing substrate was placed beneath the LSC to make sure the light only made a single pass through the partially transparent LSC. This configuration would mimic an IGU that does not have any other coatings on the inside of a window, and the QDs would only absorb the incident sunlight. The second configuration used a mirror beneath the LSC in order to simulate a low-e coating that most commercial IGUs have on an inner surface of a double-pane window. Low-e

coatings are regularly used to control the heat gain through the window by reflecting NIR light (typically wavelengths > 750 nm) incident on the window, but because most low-e coatings are thin films of metal, some of the visible light is reflected as well. This light can then be absorbed by the LSC and boost its performance.

The I - V curves and respective EQE curves are shown in Figure 2c,d, respectively. A measured PCE for the nonreflective substrate is 2.18% and increases to 2.94% when the reflective substrate is used (see the Supporting Information for more electrical characterization). These PCE values indicate that the device could produce ~ 22 – 30 W/m² (with a VLT of 44%), depending on what additional coatings were on the IGU, while, ultimately, the target performance is >50 W/m² with a VLT of 50%, as discussed below.

In order to determine if a target power production of 50 W/m² is a viable benchmark to enable a short payback for tall buildings, we modeled the power generation of various heights of tall buildings equipped with LSCs for five different U.S. cities. To model the annual electricity production of these buildings, we assumed that the windows were equipped with 5% efficient solar cells that transmitted 50% of the solar spectrum (see the Supporting Information for more details).

For each building, we varied the number of stories and the percentage of the glass on the building façade and calculated the annual electricity production using the “typical meteorological year” weather data for each city's representative climate zone (Figure 3). The results from this simulation show that at a

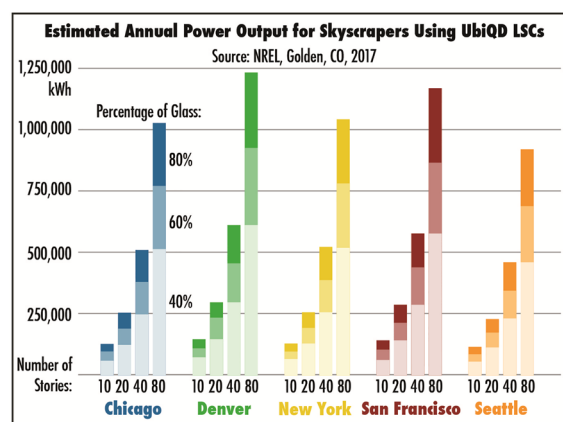


Figure 3. Estimated annual power output for buildings using NIR-QD laminated glass LSCs with a power output of 50 W/m² at 50% transmittance.

target output of 50 W/m² an 80 story building could produce over 1 GWh of electricity annually, which would offset \sim \$200K in annual electricity for a building located in New York, for example.

Although the performance of the LSCs presented in this study is only about halfway to the target, there are several pathways to improve their characteristics. First, we observe a low PCE value of 2.18% (single pass) compared to the 8.1% measured optical efficiency. However, the optical efficiency does not account for the coupling losses into the edge-attached solar cell nor the solar cell PCE. In this Letter, we did not optimize the solar cells type or their geometry for use with the LSC. For example, the cells used in this study were twice as wide as the LSC thickness, which resulted in significant shading of the solar cells. Further, as mentioned above, the solar cell

PCE was only $\sim 11\%$ (based on the full area, not the active area), which is low compared to high-performance Si solar cells or GaAs cells used in some other works. The efficiency of converting the quasi-monochromatic QD emission (centered at 880 nm) should be higher than the PCE, possibly more than double,²⁷ although we did not measure it directly. Somewhat nonuniform coverage of the LSC edges by epoxy could affect optical coupling to the solar cells and thus reduce the overall PCE. Clearly, optimization of the form factor of the solar cells as well as minimization of the haze are required to improve performance of the LSCs. Utilizing higher PCE solar cells with an optimized geometry, improving the edge optical coupling, reducing nanocomposite haze, and increasing the LSC's sunlight absorption should enable future prototypes to exceed 50 W/m².

In conclusion, laminated glass QD LSCs for electricity generation on building façades are an attractive means to realize net-zero power consumption for modern cities. LSC prototypes enabled by high-QY, NIR-emitting CuInS₂/ZnS QDs were demonstrated with a record high optical efficiency of 8.1% and certified champion PCE of 2.94%. With further optimization, laminated glass LSCs have the potential to disrupt the urban energy landscape by offering seamless low-cost integration of energy production into the façades of buildings.

■ ASSOCIATED CONTENT

Supporting Information

The Supporting Information is available free of charge on the ACS Publications website at DOI: 10.1021/acsenenergylett.7b01346.

Theoretical limitations of LSCs, optical properties of glass laminate LSCs and QDs discussed in the main text, effect of different glass types, and details of the device certification (PDF)

■ AUTHOR INFORMATION

Corresponding Author

*E-mail: hunter@ubiqd.com. Tel: 505-310-6766.

ORCID

Hunter McDaniel: 0000-0002-5009-918X

Author Contributions

§M.R.B. and N.S.M. contributed equally.

Notes

The authors declare the following competing financial interest(s): The authors declare a financial interest, in some cases exceeding 5%, in their affiliated corporate institution, UbiQD, Inc., which may benefit from the publication of this Letter. Among the potential benefits to UbiQD, Inc. is the increased perceived value of intellectual property that the company owns or exclusively licenses. Specifically, the company has filed patents on laminated glass luminescent solar concentrators and licenses earlier patents on luminescence solar concentrators and quantum dot materials.

■ ACKNOWLEDGMENTS

This material is based upon work supported by the National Science Foundation under the phase I small business innovation and research (SBIR) Grant No. 1622211. This material is based upon work supported by the U.S. Department of Energy, Office of Science, Office of Energy Efficiency and

Renewable Energy via the Small Business Vouchers Pilot Program under Award Number CRD-16-640.

■ REFERENCES

- (1) Brunisholz, M. J. *IEA-PVPS Annual Report 2016*; Imprimerie St-Paul: Fribourg, Switzerland, 2017; ISBN 978-3-906042-63-3.
- (2) Howard, B.; Parshall, L.; Thompson, J.; Hammer, S.; Dickinson, J.; Modi, V. Spatial Distribution of Urban Building Energy Consumption by End Use. *Energy and Buildings* **2012**, *45*, 141–151.
- (3) Monthly Electric Sales and Revenue With State Distributions Report. U.S. Energy Information Administration (EIA), Department of Energy, Form EIA-860; June 2017.
- (4) Stahl, W.; Zastrow, A. Fluoreszenzkollektoren. *Phys. Unserer Zeit* **1985**, *16*, 167–179.
- (5) Meinardi, F.; Bruni, F.; Brovelli, S. Luminescent Solar Concentrators for Building-Integrated Photovoltaics. *Nat. Rev. Mater.* **2017**, *2*, 17072.
- (6) Weber, W. H.; Lambe, J. Luminescent Greenhouse Collector for Solar Radiation. *Appl. Opt.* **1976**, *15*, 2299–2300.
- (7) Goetzberger, A.; Greubel, W. Solar Energy Conversion with Fluorescent Collectors. *Appl. Phys.* **1977**, *14*, 123–139.
- (8) Ippen, E. P.; Shank, C. V.; Dienes, A. Rapid Photobleaching of Organic Laser Dyes in Continuously Operated Devices. *IEEE J. Quantum Electron.* **1971**, *7*, 178–179.
- (9) Beer, D.; Weber, J. Photobleaching of Organic Laser Dyes. *Opt. Commun.* **1972**, *5*, 307–309.
- (10) Bomm, J.; Büchtemann, A.; Chatten, A. J.; Bose, R.; Farrell, D. J.; Chan, N. L. A.; Xiao, Y.; Slooff, L. H.; Meyer, T.; Meyer, A.; et al. Fabrication and Full Characterization of State-of-the-Art Quantum Dot Luminescent Solar Concentrators. *Sol. Energy Mater. Sol. Cells* **2011**, *95*, 2087–2094.
- (11) Barnham, K. W. J.; Marques, J. L.; Hassard, J.; O'Brien, P. Quantum-Dot Concentrator and Thermodynamic Model for the Global Redshift. *Appl. Phys. Lett.* **2000**, *76*, 1197–1199.
- (12) Chatten, A. J.; Barnham, K. W. J.; Buxton, B. F.; Ekins-Daukes, N. J.; Malik, M. A. Quantum Dot Solar Concentrators. *Semiconductors* **2004**, *38*, 909–917.
- (13) Chin, P. T. K.; de Mello Donega, C.; van Bavel, S. S.; Meskers, S. C. J.; Sommerdijk, N. A. J. M.; Janssen, R. A. J. Highly Luminescent CdTe/CdSe Colloidal Heteronanocrystals with Temperature-Dependent Emission Color. *J. Am. Chem. Soc.* **2007**, *129*, 14880–14886.
- (14) Shcherbatyuk, G. V.; Inman, R. H.; Wang, C.; Winston, R.; Ghosh, S. Viability of Using Near Infrared PbS Quantum Dots as Active Materials in Luminescent Solar Concentrators. *Appl. Phys. Lett.* **2010**, *96*, 191901–191904.
- (15) Meinardi, F.; McDaniel, H.; Carulli, F.; Colombo, A.; Velizhanin, K. A.; Makarov, N. S.; Simonutti, R.; Klimov, V. I.; Brovelli, S. Highly Efficient Large-Area Colourless Luminescent Solar Concentrators using Heavy-Metal-Free Colloidal Quantum Dots. *Nat. Nanotechnol.* **2015**, *10*, 878–885.
- (16) Meinardi, F.; Ehrenberg, S.; Dharmo, L.; Carulli, F.; Mauri, M.; Bruni, F.; Simonutti, R.; Kortshagen, U.; Brovelli, S. Highly Efficient Luminescent Solar Concentrators Based on Earth-Abundant Indirect-Bandgap Silicon Quantum Dots. *Nat. Photonics* **2017**, *11*, 177–185.
- (17) Klimov, V. I.; Baker, T. A.; Lim, J.; Velizhanin, K. A.; McDaniel, H. Quality Factor of Luminescent Solar Concentrators and Practical Concentration Limits Attainable with Semiconductor Quantum Dots. *ACS Photonics* **2016**, *3*, 1138–1148.
- (18) Sumner, R.; Eiselt, S.; Kilburn, T. B.; Erickson, C.; Carlson, B.; Gamelin, D. R.; McDowall, S.; Patrick, D. L. Analysis of Optical Losses in High-Efficiency CuInS₂-based Nanocrystal Luminescent Solar Concentrators: Balancing Absorption Versus Scattering. *J. Phys. Chem. C* **2017**, *121*, 3252–3260.
- (19) Li, L.; Pandey, A.; Werder, D. J.; Khanal, B. P.; Pietryga, J. M.; Klimov, V. I. Efficient Synthesis of Highly Luminescent Copper Indium Sulfide-Based Core/Shell Nanocrystals with Surprisingly Long-Lived Emission. *J. Am. Chem. Soc.* **2011**, *133*, 1176–1179.
- (20) McDaniel, H.; Koposov, A. Y.; Draguta, S.; Makarov, N. S.; Pietryga, J. M.; Klimov, V. I. Simple Yet Versatile Synthesis of

CuInSe_xS_{2-x} Quantum Dots for Sunlight Harvesting. *J. Phys. Chem. C* **2014**, *118*, 16987–16994.

(21) Slooff, L. H.; Bende, E. E.; Burgers, A. R.; Budel, T.; Pravettoni, M.; Kenny, R. P.; Dunlop, E. D.; Büchtemann, A. A Luminescent Solar Concentrator with 7.1% Power Conversion Efficiency. *Phys. Phys. Status Solidi RRL* **2008**, *2*, 257–259.

(22) Wu, K.; Li, H.; Klimov, V. I. Tandem Luminescent Solar Concentrators Based on Engineered Quantum Dots. *Nat. Photonics* **2018**, *12*, 105.

(23) Li, H.; Wu, K.; Lim, J.; Song, H.-J.; Klimov, V. I. Doctor-Blade Deposition of Quantum Dots onto Standard Window Glass for Low-Loss Large-Area Luminescent Solar Concentrators. *Nat. Energy* **2016**, *1*, 16157.

(24) Zhao, H.; Benetti, D.; Jin, L.; Zhou, Y.; Rosei, F.; Vomiero, A. Absorption Enhancement in “Giant” Core/Alloyed-Shell Quantum Dots for Luminescent Solar Concentrator. *Small* **2016**, *12*, 5354–5365.

(25) Zhou, Y.; Benetti, D.; Fan, Z.; Zhao, H.; Ma, D.; Govorov, A. O.; Vomiero, A.; Rosei, F. Near Infrared, Highly Efficient Luminescent Solar Concentrators. *Adv. Energy Mater.* **2016**, *6*, 1501913.

(26) Meinardi, F.; Colombo, A.; Velizhanin, K. A.; Simonutti, R.; Lorenzon, M.; Beverina, L.; Viswanatha, R.; Klimov, V. I.; Brovelli, S. Large-Area Luminescent Solar Concentrators Based on ‘Stokes-Shift-Engineered’ Nanocrystals in a Mass-Polymerized PMMA Matrix. *Nat. Photonics* **2014**, *8*, 392–399.

(27) Green, M. A.; Zhao, J.; Wang, A.; Wenham, S. R. 45% Efficient Silicon Photovoltaic Cell under Monochromatic Light. *IEEE Electron Device Lett.* **1992**, *13*, 317–318.